relyon plasma

Attracting Tomorrow TDK

piezobrush® PZ3:
Part I: Operation Principle and Characteristics

Dariusz Korzec, Florian Hoppenthaler, Thomas Andres,
Dominik Burger, Andrea Werkmann, Stefan Nettesheim,
and Markus Puff

October, 2020

Outline

The **subject** of this whitepaper is the atmospheric pressure plasma jet piezobrush® PZ3, developed by Relyon Plasma GmbH in Regensburg, Germany, on the base of the CeraPlas® F and CeraPlas® drive - both products of TDK Electronics GmbH & Co OG in Deutschlandsberg, Austria.

The main task of the piezobrush® PZ3 is the plasma treatment of different materials for increase of the surface energy. The increased surface energy enhances the wettability, the adhesion of glues, casting compounds and sealings or improves the printability in wide range of industries. The treatment rate in the range of few square centimeters per second makes the piezobrush® PZ3 predestined for small-scale works mainly in the laboratory, workshop, and small-scale production. The low thermal load makes it possible to apply the piezobrush® PZ3 in combination with specialized nozzles on biomaterials and tissues.

The **objective** of this document is the technical presentation of the piezobrush® PZ3 addressed to potential technical sales and users. The document contains a short explanation of the working principles, comparison to other plasma tools, typical applications, technical and performance data. The comparison was made with the predecessor device piezobrush® PZ2. The presented information should help in deciding the specific applications the device can be used for. The measurement of Ozone concentration, electric field and activation area have been used for the quantitative characterization of the piezobrush® PZ3. The piezobrush® PZ3 whitepaper Part II and III deal with principles, performance characterization, and application examples of specialized nozzles.

Keywords: atmospheric pressure plasma jet (APPJ), piezoelectric direct discharge (PDD), piezoelectric transformer (PT), CeraPlas® F, plasma surface treatment

1 Introduction

The piezoelectric transformers (PTs) [9] of Rosen type [45] were broadly used as a high voltage source for power electronics [7, 32]. The specification of such PTs allowed for the ignition of low-pressure gaseous discharges, such as neon lamps [46], cold cathode fluorescent lamps (CCFL) [58, 33], oxygen containing gas mixtures for Ozone generation [27, 52] or plasma for thrusters [23]. The resonantly driven PTs [4] with multilayer structure [22] reached voltage transformation ratios sufficient for sustaining a high intensity atmospheric pressure plasma jets (APPJs) with noble gases [34, 55, 56, 53, 54, 29, 15].

Reinhausen Plasma GmbH (the predecessor of Relyon Plasma) commercialized desktop device belonging to this generation under brand name piezobrush® PZ1 in 2009. It generates an efficient discharge in helium and is a useful tool for surface activation before processing steps such as: gluing, painting, printing, casting, foaming, coating or siliconizing. An increase of wettability, printability or adhesion has been achieved on polymers [40, 48, 41], silica [28], and ceramics. [25, 26]

The specialized plasma generating device CeraPlas® F, working with low input voltage in the range of 5 – 25 V, and being able to work with environmental air as a plasma gas due to high voltage transformation ratio (see section 4.1), was developed by EPCOS in Deutschlandsberg [50]. The CeraPlas® F has no high voltage electrode, but the entire high voltage PZT surface is used for plasma ignition. This novel method of plasma generation is called piezoelectric direct discharge (PDD) [59]. The CeraPlas® F enabled the development of the world-wide first hand-held piezoelectric device generating plasma with environmental air [39]. Starting from 2014, this device was commercialized by Relyon Plasma GmbH as piezobrush® PZ2. It is distributed over a world-wide network of sales partners and is also labeled for OEM customers. The piezobrush® PZ3 is a further development of piezobrush® PZ2 based on the same CeraPlas® F and novel driver elec-

tronics.

2 Applications of piezobrush® PZ2

The piezobrush® PZ2 covers all application fields of the piezobrush® PZ1 and enables many new applications. The representative examples are the treatment of polymer surfaces for improvement of printability, adhesion and casting [8] and the pretreatment (cleaning, activation) of titanium [57] for implantology. Due to a moderate **activation rate** of 2-5 cm^2/min, the piezobrush® PZ2 is applied mainly in research and development labs, workshops and production sites for small components such as sockets, plugs or wire ends. In course of commercialization, different features were added to the original piezobrush® PZ2 device for fulfillment of the customer's wishes. The near-field nozzle allows a safe operation with electrically conductive substrates (metals, carbon reinforced plastics, carbon containing rubbers). The multi-gas-nozzle allows the operation with noble gases, the operation with noble gas mixtures with molecular gases and with nitrogen. The needle nozzle allows a precise plasma-thermal micro-treatment. To address the needs of industrial users, the piezobrush® PZ2-i version was developed, allowing an external switching of the plasma and an application of the clean gases: compressed dry air (CDA) or nitrogen. If using the flow control, the CeraPlas® F cooling conditions in piezobrush® PZ2-i are independent on the type of nozzle or the substrate distance.

3 piezobrush® PZ3

Based on the extended application and service experience with piezobrush® PZ2 collected since 2014, the model piezobrush® PZ3 (see figure 1) was developed as a result of cooperation of TDK-Electronics (ex-Epcos) and Relyon Plasma GmbH.

3.1 The new features of the piezobrush® PZ3

The piezobrush® PZ3 is, similarly to piezobrush® PZ2, a hand-held device working with environmental air and applying the same CeraPlas® F. The main technical innovations of the piezobrush® PZ3 in comparison with the piezobrush® PZ2 are:

- **Intelligent replaceable modules.**

  The fully operable piezobrush® PZ3 consists of an ac-dc power adapter supplying 24 V, a base unit comprising a fan and electronic boards and a replaceable CeraPlas® F module (see figure 2). The main component of each CeraPlas® F module is the CeraPlas® F fixed in a plastic holder. For easy replacement, the CeraPlas® F module is equipped with a contact strip which fits in a CeraPlas® F module socket located on the human machine interface (HMI) board. This multi-task connection supplies the 50 kHz voltage to the CeraPlas® F input and allows the reading/writing of relevant information in the CeraPlas® F module. During operation, the operating hours counter is actualized. Important operating conditions such as sensor values (temperatures, acceleration, current) are recorded for diagnostics purposes. The stored information about the CeraPlas® F module type is used by the system controller to set the proper operating conditions for the specific nozzle integrated in the CeraPlas® F module. Storing the operation settings in the CeraPlas® F module allows for an easier adoption of the future specialized nozzles. The integration of the CeraPlas® F in each replaceable CeraPlas® F module allows for smaller admissible tolerance of the distance between the CeraPlas® F tip and the coupling electrode in the near-field nozzle and the multi-gas nozzle. This tolerance is essential for reproduceable process results and a stable plasma intensity. An additional advantage of modularity is an easier servicing of the device, especially the replacement of the CeraPlas® F.

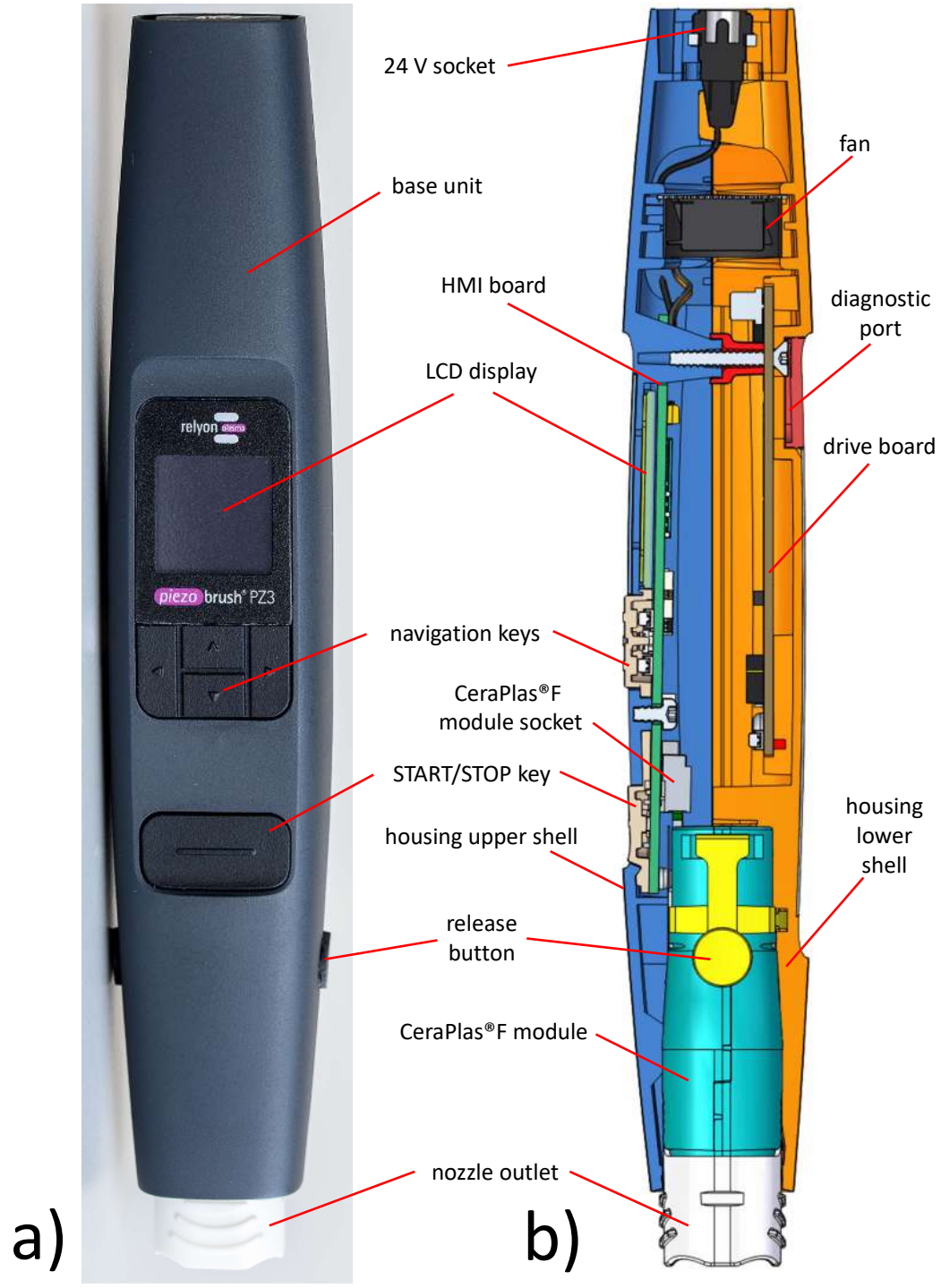

Figure 1: Front view a) and side view cross-section b) of the piezobrush® PZ3.

- **Human-machine-interface.**

  The only operation function of the piezobrush® PZ2 is switching on and off by use of a single key. The piezobrush® PZ3 can also be used like this, but has much more versatile user options, which are realized by use of a HMI interface. The printed circuit board (PCB) of the HMI is integrated in the housing upper shell. The HMI comprises a 64 × 80 color OLED display, four arrow keys and a START/STOP key (see figure 1 (a)). The arrow keys allow for the navigation in the user menu and selection of the parameter settings. The user can choose different operation modes and settings. The HMI functions are described in the next section.

- **Powerful drive board.**

  Similar to the piezobrush® PZ2 drive, the CeraPlas® drive comprises the system controller and CeraPlas® F signal management circuitry. The aim of the increased computing power of the new CeraPlas® drive is the extended device diagnostics, better frequency control and communication with the HMI board. The sinusoidal excitation signal of the CeraPlas® F can be generated. The 24 V ac-dc adapter instead of 15 V one is used to power the piezobrush® PZ2 drive.

- **Plasma and device diagnostics.**

  Two levels of plasma and device diagnostics are implemented. The first level, accessible for the user, is over the HMI interface, with warnings and failures described in section 3.2. The second level, accessible over a diagnostic port (see figure 1), can be used for service purposes.

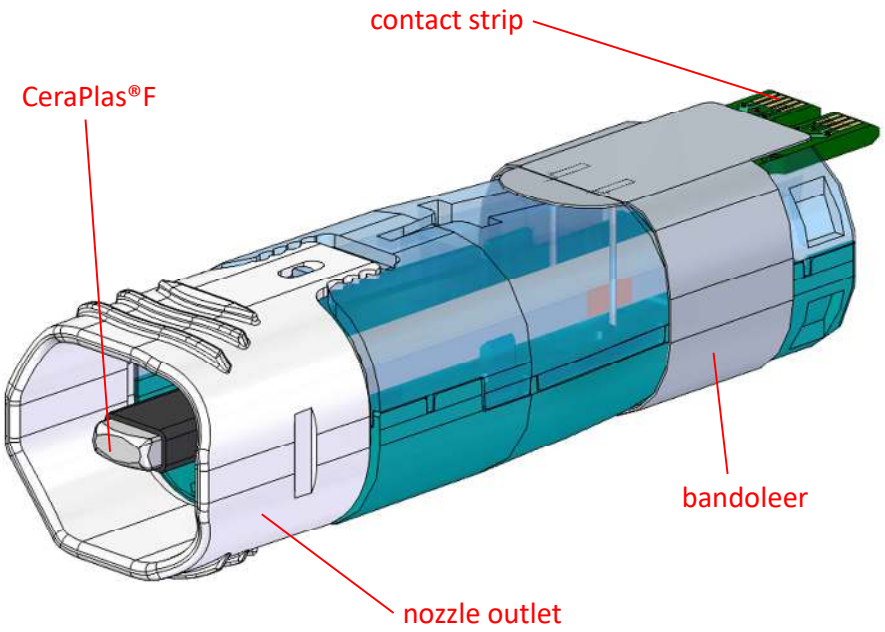

Figure 2: The replaceable CeraPlas® F open nozzle module used in piezobrush® PZ3.

- **Optimized fan.**

  A fan with a magnetic bearing and a brushless motor, and consequently with the increased lifetime of 70,000 hours, the reduced power consumption of 0.53 W, and reduced noise is used. The implementation of the 5 V supply allowed to apply a very compact fan with an optimal aerodynamic characteristic. The reduced air flow results in a higher efficiency of the surface treatment (see section 6.2 for explanation). At the same time, it is sufficient for cooling of the CeraPlas® F and the electronic PCBs in the piezobrush® PZ3 housing. The reduced power consumption of the fan allows for longer operation time if used with a battery pack.

- **Novel mechanical features.**

  The main mechanical properties (sizes, weight, overall shape) are similar to those of the piezobrush® PZ2. A robust, close tolerated mechanism with release buttons is implemented in the piezobrush® PZ3 for locking the CeraPlas® F modules. The

design of the plasma generating part of the piezobrush® PZ3 prevents the device from being too close to the electrically conducting objects as described in detail in operation manual [44]. This measure minimizes the risk of a spark to the fingers of the operator or metal tools and reduces the failure probability of the CeraPlas® F. A better look of the device case is reached by the up-to-date design and an improved polymer surface finish.

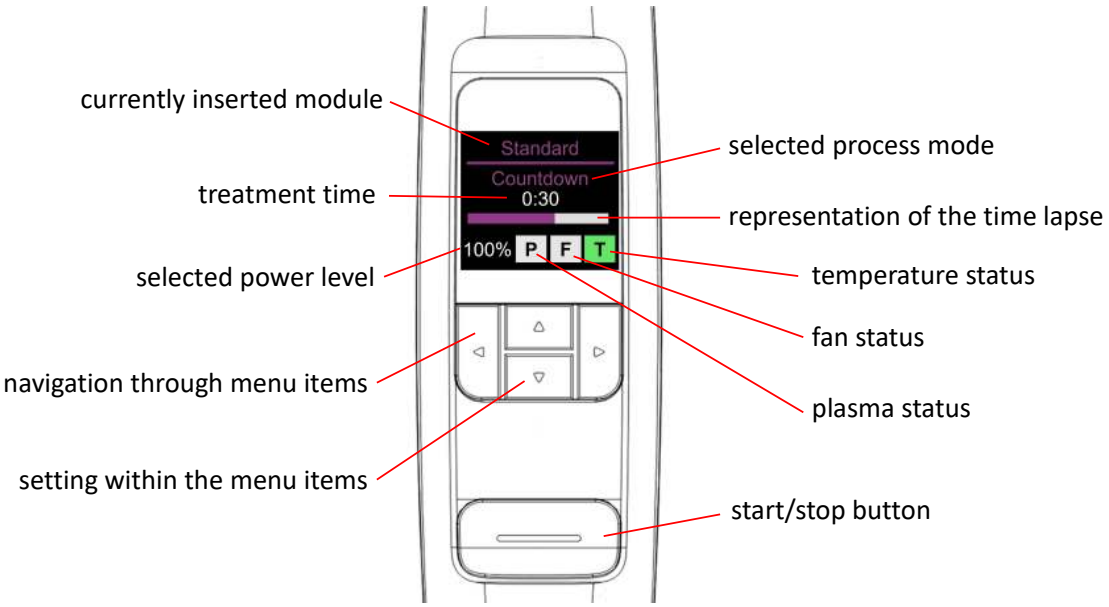

Figure 3: Display and buttons of the human-machine interface (HMI).

3.2 Functions of the HMI

The piezobrush® PZ3 is equipped with an extended intelligence and flexibility, which are accessible and controllable by the HMI. The HMI display contents and the function of the buttons is explained in figure 3. In following, the most important features of this HMI are shortly described.

Plug and play.

After switching on the 24 V power supply (or inserting the powered plug)

- the fan starts working with the stand-by power (3 V supplied to the fan),
- the OLED display is on and in an **operation mode**, and
- the settings used before last power OFF are active.

After 3 seconds, the plasma can be switched on by use of the START/STOP key. During plasma operation the fan is working with full power (supply voltage of 5 V).

User choices

By pressing the left or right key, the HMI is switching to the menu mode, and then the selection of one of the following menu items is possible:

- process (countdown, metronome, stopwatch),
- time (from 1 s to 5 min in 1 s steps),
- power (from 30% to 100% in 5% steps),
- failure or worn handling mode,
- buzzer volume (level from 1 to 5),
- orientation of the display and the keys (portrait or landscape),
- nozzle information (max power, uptime, starting date) – no selection, and
- device information and firmware version – no selection.

The values can be set by use of the up and down keys. After 15 s without any actions, the display returns automatically to the operation mode.

What does the display show?

In the operation mode, the OLED display shows (see figure 3):

- the name of the nozzle module inserted (e.g. “standard”)
- the selected process mode (e.g. “stopwatch”)
- the magenta bar visualizing the elapsing time with different meaning, depending on

the process mode selected,

- the power level, and
- the three rectangle fields with letters P, F and T.

P field shows the plasma conditions. It is white, if plasma is not switched on, it is green when plasma is ignited and OK, it turns red if open nozzle module is operated with electrically conducting objects and the power is switched off (failure). It turns orange, if the near-field plasma module is operated without conducting load for longer than 5 seconds (to avoid overheating of the CeraPlas® F) and power is switched off (failure).

F field shows the condition of the fan. White background means, that fan is running in stand-by mode. The rectangle background turns green, if plasma is switched on and the fan is operated with full power.

T field displays the thermal conditions of the electronics. Under normal conditions, it is green and in case of overheating, it turns red.

Three tools in one

The three possible process modes allow using the piezobrush® PZ3 optimally for very different tasks.

The **"stopwatch" mode** is suitable for processing of substrates with complex shapes or large areas, when the exact treatment time cannot be predicted. The elapsed time is displayed without magenta bar visualization. The plasma remains ON until the next pressing of the START/STOP key.

The **"countdown" mode** is very useful, if a large number of substrates with the same treatment time should be processed. The magenta bar length visualizes the remaining plasma-ON time. When the countdown time is elapsed, a buzzer sound signalizes the end

of the plasma operation. The fan returns to the "stand-by" mode.

In the **"metronome" mode**, the elapsed time is shown and visualized with the magenta bar. After reaching the set time, the bar is going to zero and a buzzer sound can be heard. The plasma is continuing to be ON. The time counting of the new cycle starts automatically. The acoustic feedback is a useful aid if larger substrates should be treated with a repeating back-and-forth motion of the piezobrush® PZ3 and each sweeping movement should have roughly the same duration.

Is this a failure?

The piezobrush® PZ3 handles in an intelligent way the untypical situations during the device operation and informs the user about such condition. For example, if no plasma module is inserted, a black display with warning "no module found" informs that no plasma can be ignited without plasma module.

If no keys are pressed longer than 1 min, the OLED display is getting darker.

The movement sensor, belonging to the controller board, is used for detection of the still stand. If the piezobrush® PZ3 is left running longer than 5 min without any motion in any process mode, the power is switched off and if motion is detected, the operation will not be interrupted.

4 The CeraPlas® F operation principle

The task of the CeraPlas® F is to generate a high ac voltage, typically over 10 kV. The electric field at the CeraPlas® F tip causes an ionization processes in the surrounding gas and the initiation of a **micro-discharge** [14]. The voltage transformation is achieved at resonant frequency due to the formation of a standing acoustic wave which transforms the low voltage from the input side to a high voltage at the mechanically coupled output side. To minimize the damping of the oscillation, the fixtures and electric connections of the CeraPlas® F are positioned in the nodal points of this standing acoustic wave. The

following sections show how the generation of high voltage and sustaining plasma can be achieved by piezoelectric principle and by control of the CeraPlas® F.

4.1 Piezoelectric principle

The main task of the CeraPlas® F is, similar to the common magnetic transformers, the conversion of the electric ac input signal with low voltage and high current to the output signal with high voltage and low current. Thereby, its performance is characterized by the **voltage transformation ratio** defined as the ratio of the output voltage to the input voltage. Essential for operation of the CeraPlas® F are two physical effects: the direct piezoelectric effect and the indirect (converse) piezoelectric effect [38]. The direct piezoelectric effect causes the increase of the polarization strength and, consequently, the surface charge density on two sides of a piezoelectric material, when it is subjected to the external mechanical stress. This effect is especially strong if the mechanical force is applied in the direction of the polarization vector in a pre-polarized ferroelectric material. The converse piezoelectric effect occurs if a mechanical deformation of the piezoelectric material follows the voltage applied on this material. Also, this effect is strongest in pre-polarized ferroelectric material blocks when the electric field is applied parallel to the vector of polarization.

The idea of the PT is to combine these two effects in a two-zones material block. In the primary zone, a small voltage is applied to induce its geometrical deformation (converse piezoelectric effect). The primary zone is mechanically connected to the secondary zone, in which the mechanical deformation of the first block is causing the mechanical stress, resulting in the generation of a high voltage. A specific technical solution is a two-zone cuboid-shaped block.

Typically, the primary zone is polarized perpendicular to the cuboid long axis and the

Table 1: The typical parameter of CeraPlas® F [50].

parameter description	parameter value
operating frequency [kHz]	50
maximum voltage transformation ratio	~ 1000
weight [g]	8.0
length x width x thickness [mm]	$72 \times 6 \times 2.8$
material	PZT
maximum operating power [W]	8.0
input voltage [V]	12 – 24
output voltage [kV]	< 15
input capacity C_{in} [μF]	$\sim$2.0
output capacity C_{out} [pF]	$\sim$3.0
Ozone production rate in air [mg/h]	< 100

same way, the voltage is applied. The secondary zone is polarized parallel to the long axis of the cuboid, causing generation of a high voltage due to the axial force from the first block. Such mechanical deformation of the input zone of the PT can be reached at much lower input voltage if multilayer structure is applied [45]. A further measure to increase the voltage transformation ratio, is using for the electric excitation signal a frequency close to the mechanical **resonance frequency**. By choosing the 2$^{\text{nd}}$ harmonic vibration mode as operation mode it is possible to contact and mount the piezoelectric transformer at the vibration nodal points without disturbing its mechanical movement. These points are also used for mechanical fixing the device.

4.2 Properties of the CeraPlas® F

The CeraPlas® F is constructed as a two-zone cuboid-shaped Rosen type, PZT (lead-zirconate-titanate [21], $\text{Pb}[\text{Zr}_x\text{Ti}_{1-x}]\text{O}_3$ $(0 \leq x \leq 1)$) based multilayer PT. The 2$^{\text{nd}}$ har-

monic frequency of a resonant longitudinal mechanical oscillation of the CeraPlas® F is used for the excitation of resonant oscillation of the PZT block. The typical parameters of the CeraPlas® F are summarized in the table 1. The formulas describing the dependence of the resonant frequency, the voltage transformation ratio and other electric properties of a PZT based PT on geometrical and material data are described in [19].

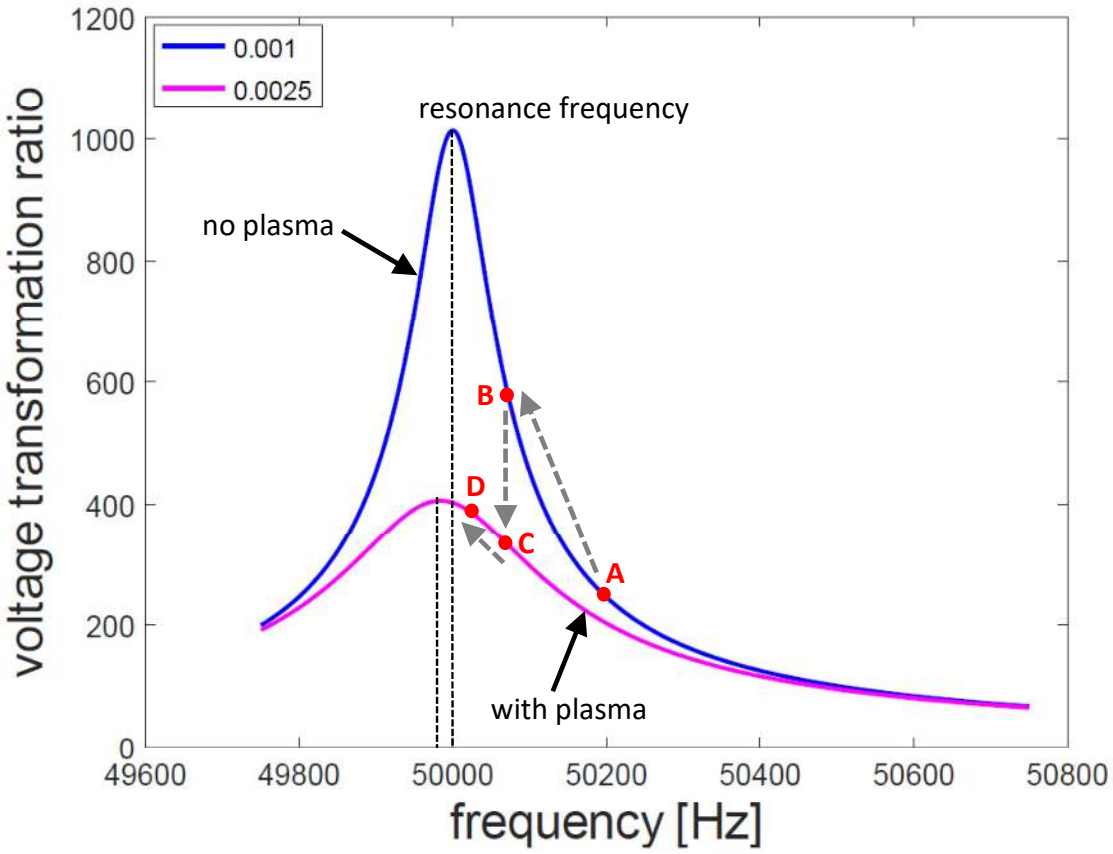

Figure 4: Trajectory of the working point of the PT on the resonant curves during plasma ignition.

4.3 CeraPlas® F as resonator

Any block of material with regular shapes has its own oscillation frequencies, like tuning fork emitting a sound with definite pitch if jolted. Also, the PZT block of the CeraPlas® F can oscillate with its own resonance frequency determined by its geometrical sizes and the material properties (speed of sound) [58] but we are not able to hear this oscillation,

because it is ultrasonic.

The behavior of a PT, considered as a **damped harmonic oscillator** [2] can be described using a resonance curve (see Figure 4) showing the dependence of the voltage transformation ratio on the excitation frequency. The voltage transformation ratio has its maximum value for resonance frequency. The resonant oscillation excited by a short input voltage pulse can continue very long or can fade away quite fast. The time constant of this decay depends on so called **damping ratio**. The ideal resonance case with the damping ratio equal zero is the endless continuing oscillation. At damping ratio values higher than 0.3, no resonant oscillation is possible (**overdamped oscillation**) [2]. For very small values of the damping ratio, the value of the oscillation amplitude at resonance frequency is high and the full width at half maximum (**FWHM**) of the resonance curve is very small. Figure 4 demonstrates the influence of the damping on the resonance curve. With increasing damping factor, in the shown example from 0.001 to 0.0025, the maximum voltage transformation ratio decreases. In the same time the FWHM increases and the resonance frequency slightly decreases. The main reasons for damping of the CeraPlas® F oscillations are:

- mechanical losses in the PZT material,
- friction of the holder system and the electric connections,
- electrostatic losses,
- capacitive coupling, and
- ohmic losses due to plasma.

4.4 Excitation frequency control

It seems easy to excite the CeraPlas® F with a frequency assuring the high voltage transformation ratio by fixing its value close to the resonant frequency. However, no stable operation can be established with constant excitation frequency. Different factors cause

variation in the resonant frequency of the device, e.g. the CeraPlas® F ambient temperature, the heating during operation and the electrical loading [31]. The frequency is changed also to control the input power, which can't be controlled directly. The power level is controlled by setting of input voltage, input current and the excitation frequency. To sustain a stable operation a fitting feedback control was implemented. Therefore, any change in the operating frequency is detected and adjusted to operate at maximum efficiency again. [16]

4.5 Plasma ignition

Figure 4 shows the operational interaction between the plasma load and the CeraPlas® F. Before the plasma ignition, the electric load of the CeraPlas® F is a small capacity, causing a weak damping. The operating point of the CeraPlas® F will be on the blue resonance curve in Figure 4 representing the low damping conditions. Since the exact plasma ignition voltage and operating frequency are not known, the starting point of the frequency control is on the right side of the resonant curve in the region of low voltage transformation ratio. This is shown as point **A**. As the operating frequency is decreased, the CeraPlas® F voltage transformation ratio moves up the "no plasma" line until the plasma ignition voltage is reached. This happens in operating point **B**. After plasma ignition, the the damping ratio increases abruptly. The ignition of plasma causes reduction of the resonant frequency and the voltage transformation ratio of the CeraPlas® F [11]. The resonance curve "no plasma" is not valid anymore. The operating point jumps to the resonance curve "with plasma" valid for stronger damping and reaches the operating point **C**. Subsequently, the operating point moves from point **C** to point **D**, causing an increase of voltage transformation ratio and consequently, plasma intensity. The operating frequency of the point **D** is reduced this way, that the input power of the CeraPlas® F can reach the set value. In the Figure 4 the plasma operation is represented by the single curve. In reality, the plasma loaded resonance curve is permanently changing, adopting its shape

to the non-constant damping ratio. The piezobrush® PZ3 firmware keeps the operating point on right side of the resonance curve to avoid control instabilities.

4.6 PDD principle

The periodic input voltage excites the oscillation of the CeraPlas® F not abruptly, but within several oscillation cycles. Depending on the mechanical vibration quality, several tens to several hundred oscillation cycles are needed to reach the output voltage value high enough for discharge ignition. During a single half-period of the voltage excitation, the multiple micro-discharges can be generated from restricted areas of the PZT surface. The output capacity plays an important role in prediction of the electric behavior of the CeraPlas® F as it consists of parallel connection of the capacity of a non-loaded CeraPlas® F (see C_{out} in table 1) and capacity of the capacitive CeraPlas® F load C_{load}. The last one varies if plasma ignites. This capacity is storing and delivering the charge needed for the evolution of the micro-discharges. The ignition of plasma is causing a decrease of the output impedance and consequently, a reduction of the resonant frequency, increase of the FWHM of the resonance curve, and decrease of the voltage transformation ratio of the CeraPlas® F.

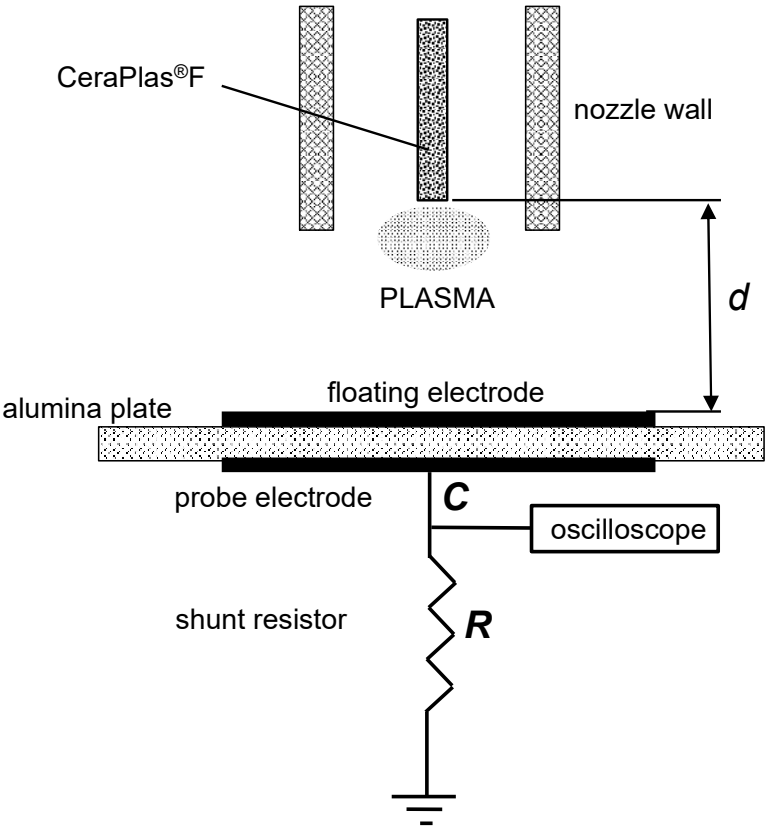

Figure 5: Principle of measurement of the electric field generated by piezoelectric discharge using capacitive large area probe, with connection for oscilloscope.

5 Characterization of the electric fields

5.1 E-field measurement

The strong electric fields generated at the tip of the CeraPlas® F can be detected by use of a capacitive probe. The one used for the PDD characterization consists of two electrodes made of a 20 μm thick aluminum foil being superimposed on both sides of a 1 mm thick alumina plate. Both electrodes are aligned and have an area of 25 cm^2. The first electrode is directed toward the CeraPlas® F and remains electrically floating. The second one is positioned on the opposite side of the Al_2O_3 plate and connected to the resistive shunt and to the oscilloscope as shown in figure 5. An optimal distance between the tip of the CeraPlas® F and the surface of the aluminum electrode is $d = 30$ mm.[1]

The measured capacity C of the capacitive probe is 187±0.2 pF. The resistor R used as a shunt, has a resistance of 9.92 kΩ. The voltage over this resistor is measured as a function of time by a voltage probe of the digital storage oscilloscope. Typically, 5000000 samples for a single measurement are collected. A duration of each sample is 0.4 ns.

5.2 E-field produced by PDD

In figure 6 the time dependent voltage signal collected from CeraPlas® F is shown. It can be considered as an overlap of a more-or-less sinusoidal, periodic line and short non-periodic pulses at the maximum and minimum of the periodic curve. The period of the sinusoidal component corresponds to the frequency of the 2nd harmonic of the resonant CeraPlas® F oscillation. This signal component is roughly proportional to the electric field on the tip of the CeraPlas® F. Both, the amplitude of the periodic signal and the number and magnitude of the micro-discharge spikes can be used for diagnostic purposes. The periodic signal component follows the changes of the electric field of the CeraPlas® F itself and can be characterized by peak-to-peak voltage value V_{pp}. This signal can be observed even if no plasma is present at the CeraPlas® F tip.

The short pulses are reactions of the capacitive probe circuitry on the field changes related to the micro-discharges at the tip of the CeraPlas® F. They are present only if the field is strong enough to cause the gaseous break-down, when the measured voltage reaches extreme values. The electric conductivity of the PZT ceramics is quite small, allowing that high voltages between different regions of the CeraPlas® F tip surface can rise. Consequently, it is possible that one region is generating already a micro-discharge, when other regions are still accumulating the charge to reach the break-down field. The consequence is that several independent micro-discharges can be ignited during a single half-period of

[1]The distance of 1.5±0.5 mm between the CeraPlas® F tip and the substrate corresponds to the position, where the substate is touching the edge of the open nozzle module (zero distance from the nozzle).

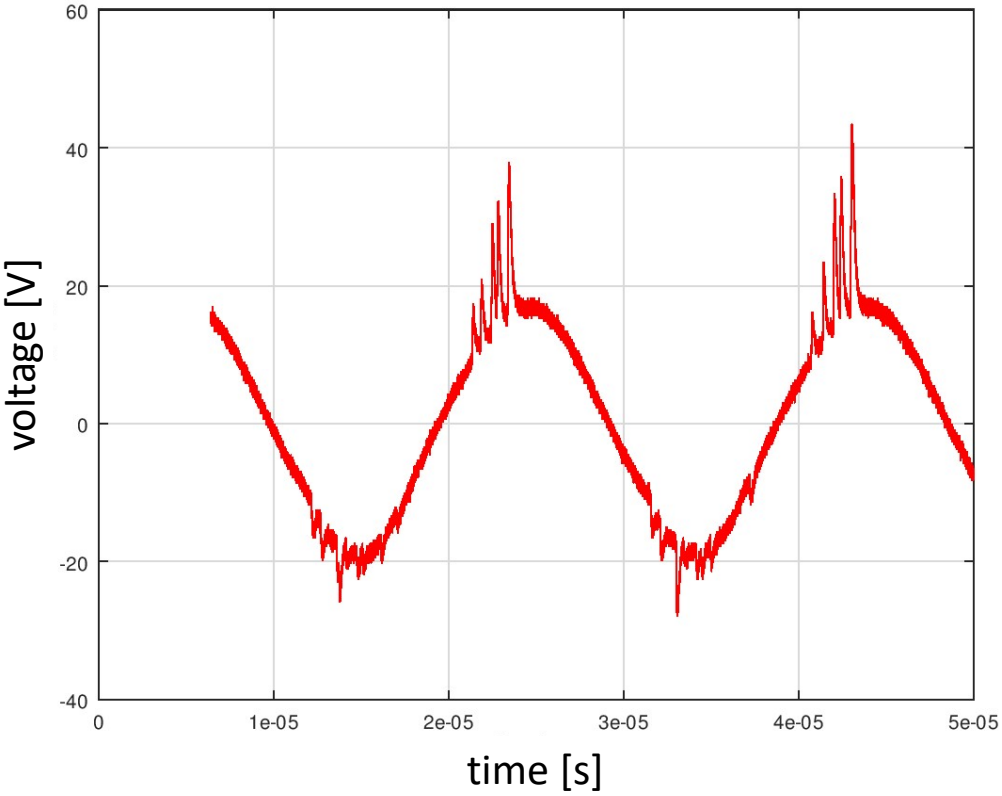

Figure 6: Voltage signal as a function of time for CeraPlas® F operated with 8.3 W power. Distance between the CeraPlas® F tip and the capacitive probe surface is 30 mm.

the CeraPlas® F oscillation.

The signals at minimum and maximum of the periodic voltage curve are different. Typically, the peaks occurring when voltage is positive (anodic peaks) are stronger than the peaks present when voltage is negative (cathodic peaks). Responsible for such asymmetry is the difference in physics of the positive and negative streamers occurring in the early phase of the micro-discharge development [30]. A positive streamer needs only a half as large electric field as a negative streamer for its propagation. It reaches also much larger dimensions than the negative one.

The higher the amplitude of the sinusoidal voltage signal, the larger the number and the

height of the micro-discharge signals. Since the micro-discharges are responsible for generation of chemically active species, their number per excitation cycle correlates with the Ozone production rate and activation efficiency.

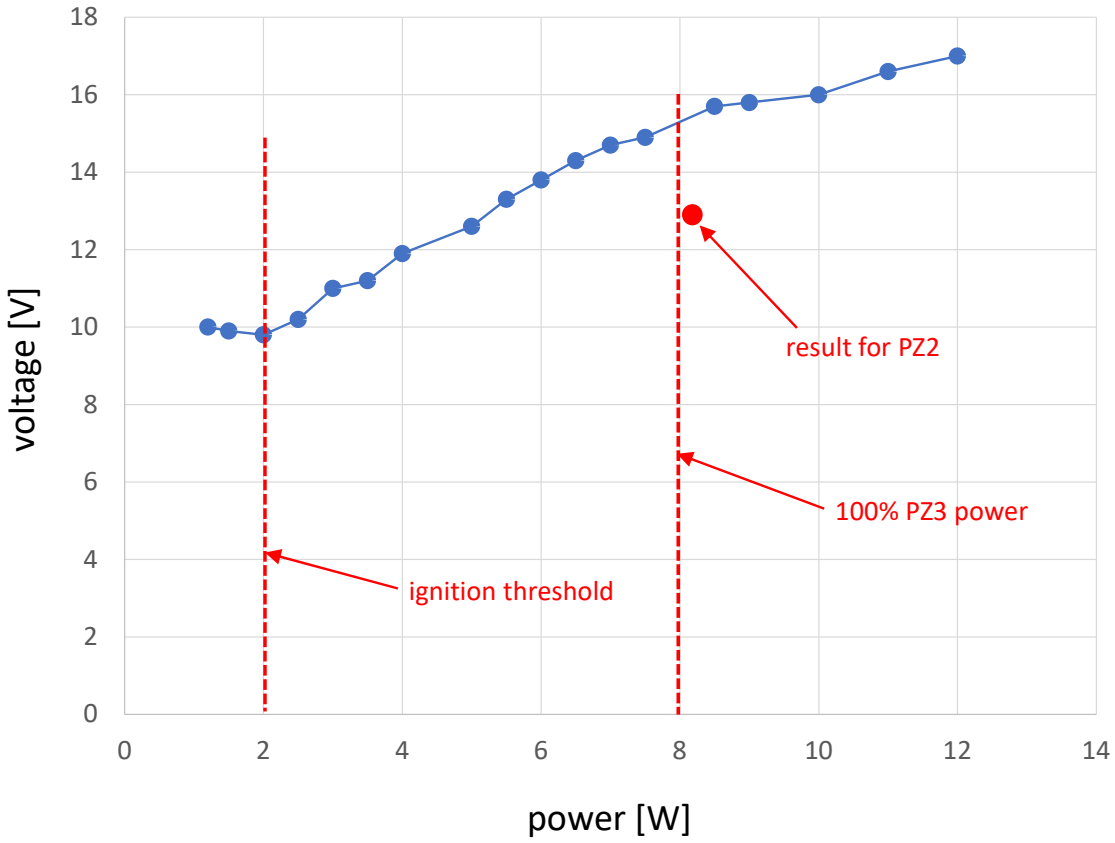

Figure 7: Amplitude of the voltage signal as a function of the CeraPlas® F input power at the electrical field measurement.

5.3 Amplitude vs. power

The amplitude of the sinusoidal component of the voltage measured by the capacitive probe is proportional to the electric field produced by a CeraPlas® F. In figure 7, the dependence of this voltage amplitude on the input power of the CeraPlas® F is displayed. For power larger than the ignition threshold, the voltage amplitude increases monotonously with power. A saturation tendency can be observed for power values over 8 W. This value corresponds to the working point of the piezobrush® PZ3, which is in the same time, the

maximum power, which can be applied to the CeraPlas® F accordingly to its specifications [51], and corresponds to the 100% power level in the HMI settings.

For comparison, the working point of the standard piezobrush® PZ2 is depicted. The voltage amplitude for piezobrush® PZ3 is approximately 20% higher than the standard piezobrush® PZ2 and this means a significant improvement of the CeraPlas® F efficiency. This improvement is due mainly to the more stable frequency control of the CeraPlas® drive in comparison with the drive of the piezobrush® PZ2. Furthermore, the fixing of the CeraPlas® F with less damping of the mechanical oscillation can contribute to better efficiency of the CeraPlas® F.

6 Ozone production

The gaseous discharge in air produces large number of chemically active and excited species [13]. They play a crucial role in all chemical reactions between plasma and the treated surface. Therefore, it is advantageous to maximize their concentrations. The most of them is short leaving, in the ns to μs range, and consequently, quite difficult for quantitative analysis. One comparatively stable product of the cold air plasma is Ozone with a typical **half-life time (HLT)**[2] in the range of hours [36]. There exist several measurement techniques for determination of the Ozone concentration in the gas phase which can be easily implemented in the lab. Thus, it is possible to use this value as an evaluation parameter for plasma generators. Also, for CeraPlas® F systematic measurements of Ozone concentration have been conducted.

6.1 Measurement method

Due to high accuracy in broad range of Ozone concentration, the UV absorption spectroscopy is frequently used [37, 10]. Various companies offer desktop instruments allowing

[2]The HLT is defined as a time that goes by until the half of the starting Ozone amount in a closed space is destructed.

measurements based on such principle. One of them is the ECO Sensors, Inc. For the Ozone concentration measurements presented in this work, their Ozone Analyzer Model UV-100 is used, allowing the Ozone concentration measurement in the range from 0.01 to 1000 ppm (volume).

6.2 Ozone concentration vs. air flow

In the piezobrush® PZ3 the air flow is produced by use of a fan, which makes the exact determination of the air flow difficult. To get exact values, the experiments with compressed dried air (CDA) precisely dosed by use of mass flow controller (MFC) are conducted.

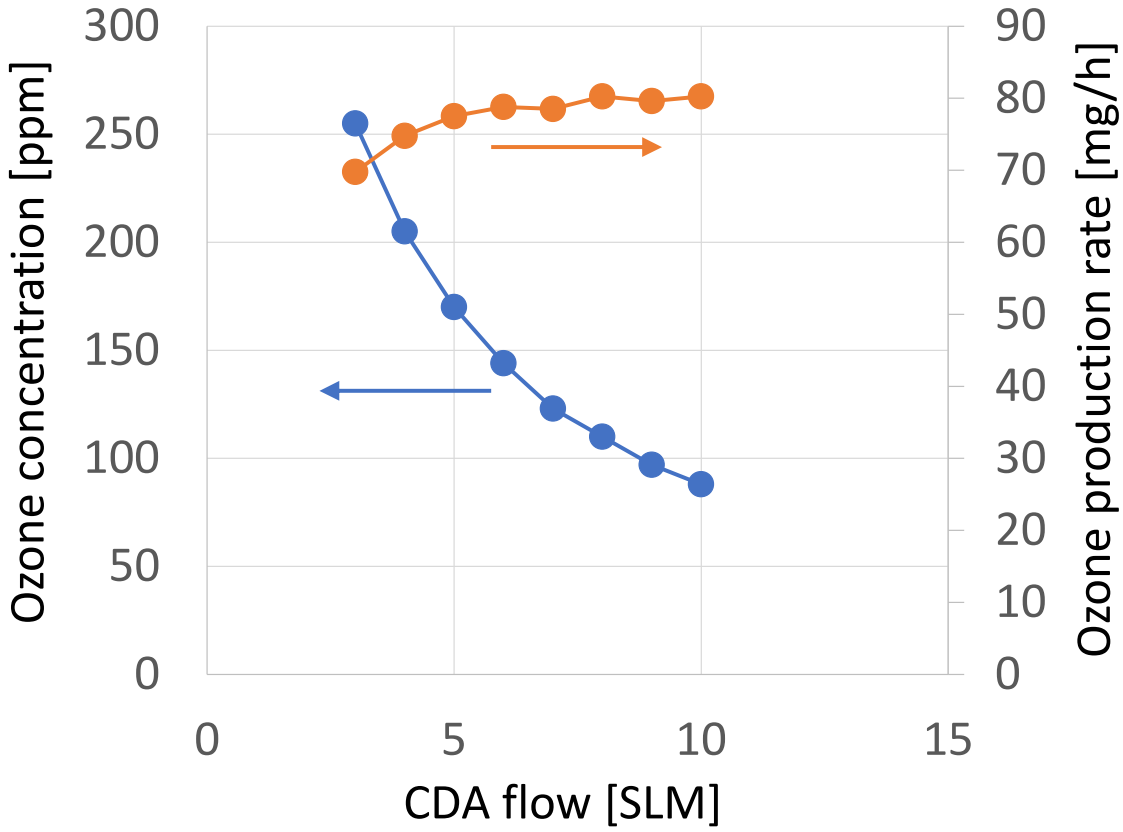

Figure 8: Concentration and production rate of Ozone as a function of CDA flow for the power of 8 W.

The concentration of Ozone as a function of CDA flow is visualized as a blue plot in

figure 8. The Ozone concentration decreases inversely proportional to the CDA flow. The increased flow causes stronger dilution of the Ozone, which reduces the process rate at the substrate. To maximize these rates, the Ozone concentration must be maximized by minimizing the air flow. The limiting factor for such minimization are the CeraPlas® F and electronics cooling requirements, which are dependent on the power coupled in the system.

6.3 Determination of the production rate

The Ozone concentration can be directly measured, but is not a suitable value for characterization of the CeraPlas® F efficiency because the result depends strongly on the air flow. A more suitable for such purpose is the production rate defined as mass of Ozone produced per time unit.

Knowing the air flow f_{air}, the production rate of Ozone R_{prod} can be calculated from the Ozone concentration N_{O_3} using following equation:

$$R_{\text{prod}} = \frac{M_{\text{O}_3}}{V_{\text{A}}} \cdot f_{\text{air}} \cdot N_{\text{O}_3} \tag{1}$$

where V_{A} is the molar volume for ideal gas[3] and M_{O_3} - the molar mass of Ozone (48 g/mol). Using the Ozone concentrations from the blue plot, the production rates are calculated and visualized as a red plot in figure 8. In the gas flow range from 5 to 10 SLM, only small variation in the production rate is observed. With gas flow decreasing below 5 SLM, the Ozone production rate decreases. This effect can be explained by the increasing temperature of the CeraPlas® F due to an insufficient air cooling. With increasing temperature following processes can affect the Ozone production rate:

(i) Changes in the CeraPlas® F itself. It is known, that with increasing temperature, the input impedance of the CeraPlas® F decreases. It means, that for the constant power, the input current increases and the input voltage decreases with temperature. The lowering of voltage results in less efficient discharge, reduction of the

[3] $V_{\text{A}} \approx 0.02479\,\text{m}^3\,\text{mol}^{-1}$ by the pressure of 100 kPa (1 bar) and temperature of 25°C.

CeraPlas® F voltage transformation ratio [49], and consequently, reduced Ozone production.

(ii) The less efficient Ozone production. An increase of specific energy input in the discharge, due to higher power or lower air flow rate, leads to an increase of concentrations of nitrogen oxides, which react with atomic oxygen - the main species needed for Ozone synthesis. This effect is known as **discharge poisoning** and can stop completely the Ozone generation [17].

(iii) The enhanced decomposition of Ozone. From 100°C upwards, the thermolysis based on reactions with radicals [3] is an increasingly important loss mechanism of Ozone.

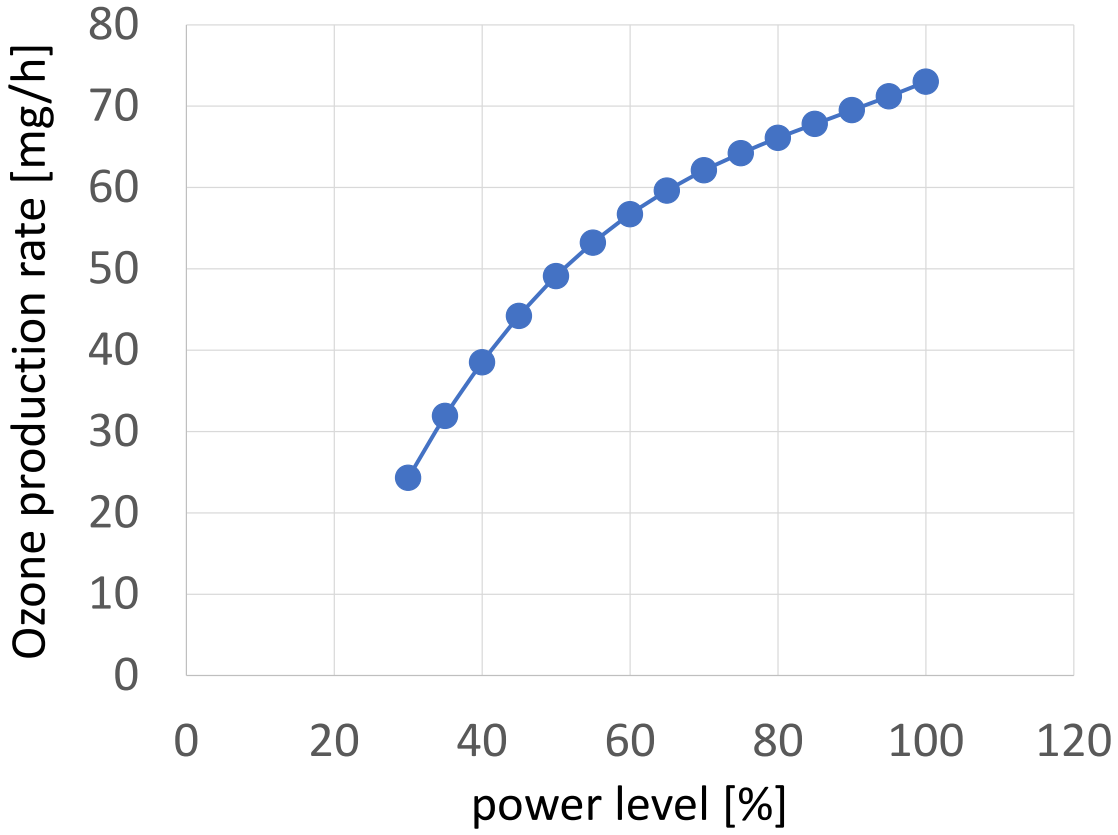

Figure 9: The Ozone production rate as a function of the piezobrush® PZ3 input power level.

6.4 Influence of power on production rate

The setting of CeraPlas® F input power level allows for wide range control of the Ozone production rate, which increases with power in the entire power level range, as shown

in figure 9. It reaches the maximum value of 73 mg/h for the highest setting of the piezobrush® PZ3 of 100% corresponding to the power of 8 W. This value, obtained with environmental air, is slightly lower, than the one shown in Figure 8 and obtained with CDA due to humidity (see the explanation in section 6.5).

A further parameter used for evaluation of Ozone production process is the Ozone **energy efficiency** defined as amount of Ozone produced per energy unit, and expressed typically in g/kWh. If the Ozone energy efficiency would not vary with increase of power coupled into the CeraPlas® F, the linear dependence between the Ozone production rate and the input power could be expected. But the dependence shown in figure 9 is not linear. The increase of the production rate is faster for lower power values (below 60%) and slows down for higher values (over 60%), which can be interpreted, as a loss of the Ozone energy efficiency with power. Reason is the increasing CeraPlas® F and discharge temperature as explained in section 6.3.

6.5 Ozone concentration in closed volume

For safety reasons or for a better plasma process control it is useful to predict the ozone concentration after some specific piezobrush® PZ3 operation time in a closed volume V. Assuming a constant production rate R_{prod}, the mean Ozone concentration $N_{\mathrm{O_3}}$ reached after piezobrush® PZ3 operation time of t can be expressed as:

$$N_{\mathrm{O_3}}(t) = \frac{R_{\mathrm{prod}}}{V} \cdot t \tag{2}$$

It means, that for example, in a not ventilated office room with a volume 3 m × 3 m × 3 m = 27 m^3 the Ozone concentration reaches the threshold for smog alarm of 180 μg/m^3 after

$$t = 180\ \mu\mathrm{g/m^3} \cdot \frac{27\ \mathrm{m^3}}{80\ \mathrm{mg/h}} \approx 4\ \mathrm{min.} \tag{3}$$

For simplicity, the equation (2) does not take the Ozone **destruction rate**[4] into account, because under typical working conditions it is quite low. At the temperature of 24°C and the relative humidity of 45%, the HLT of Ozone is 11 hours [36].

This assumption is valid for moderate Ozone concentrations reached in dry environment without factors enhancing Ozone destruction. To factors reducing the HLT of Ozone belong:

- high humidity contributing to Ozone destruction due to chemical reactions with OH and and HO_2 radicals [18],
- elevated temperature (see discussion in section 6.3),
- presence of surfaces containing water solutions with high pH-values [20, 47],
- presence of carbon [43] and some organic substances,
- presence of catalytic materials such as metalls and metallic oxides [1], especially MnO_2 [12],
- UV illumination in the wavelength range causing photolysis [35], and
- high Ozone concentration activating more efficient reaction channels for Ozone destruction.

7 Surface activation

The electric field as well as the Ozone production rate gives a valuable, but indirect information about the piezobrush® PZ3 operation. However, the process efficiency is what counts for the user. Since the most frequent applications of the piezobrush® PZ3 are related to the increase of the surface energy, two factors are of importance: (i) the maximal reached surface energy and (ii) the activation rate, which means the area with increased surface energy divided by the treatment time.

The standard method for surface energy measurement is the droplet test conducted with at

[4]The destruction rate is interpreted as a negative production rate given in g/h.

least two test liquids [5]. Other method is by use of the test inks calibrated for different surface energies, typically in steps of 2 mN/m. When using the piezobrush® PZ3 for surface activation, in very short time the maximum surface energies are reached, and it is difficult to use these values for quantitative characterization of the APPJ performance. Much more suitable for quantitative evaluation is the area of the activated surface.

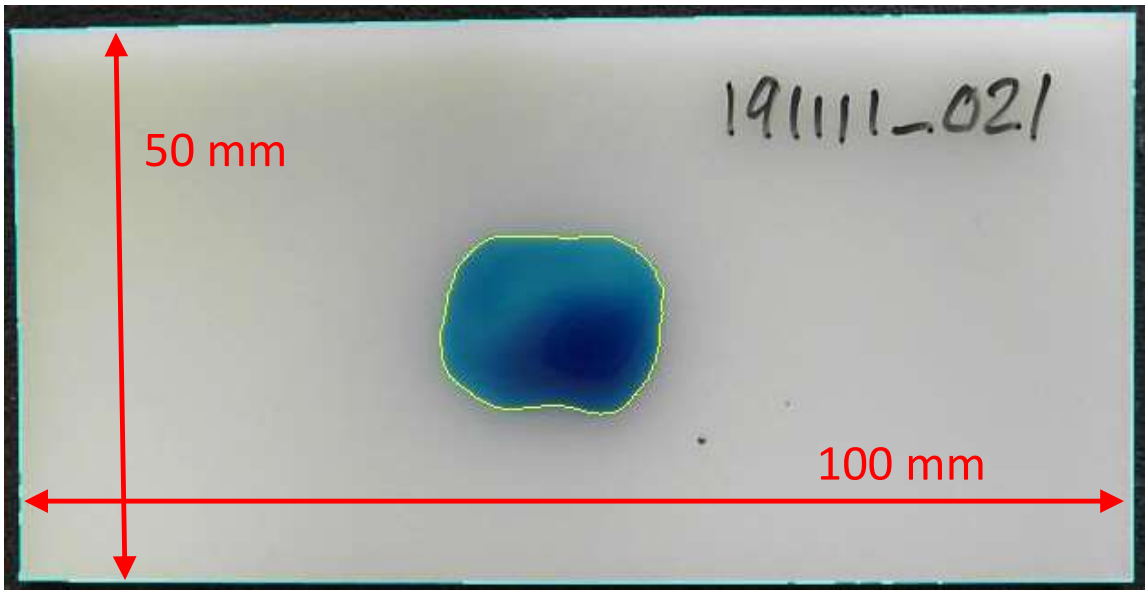

Figure 10: The plasma treated area visualized on the HDPE plate by use of a 58 mN/m test ink.

The method applied in this work is based on the measurement of the plasma treated area visualized on the HDPE plates by use of a 58 mN/m test ink (see an example in figure 10). In the following sections the activation area evaluation method and its application for characterization of the piezobrush® PZ3 are presented.

7.1 Determination of the activation area

The reasons for the choice of HDPE for plasma treatment are: (i) its high popularity and frequent use as model material for plasma activation [6], and (ii) a weak **hydrophobic recovery**. Our measurements by use of a Krüss droplet test instrument show that the surface energy reached after plasma treatment remains practically unchanged after 4 hours in environmental air.

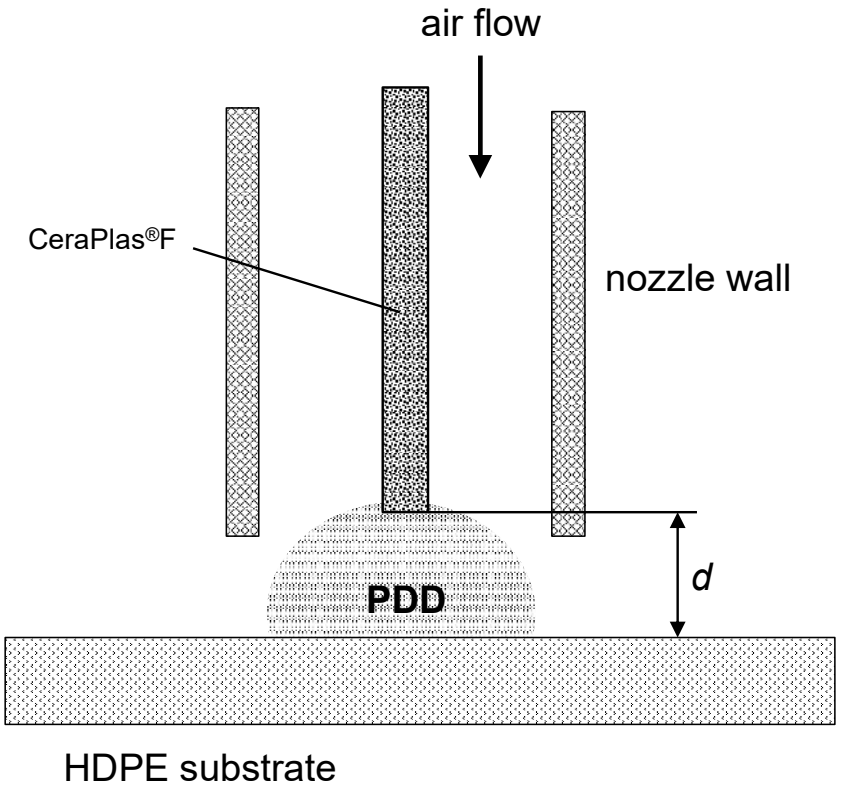

Figure 11: Setup for activation of the HDPE substrate.

For plasma treatment, the piezobrush® PZ3 is fixed and the substrate is positioned by use of a soft distance piece (e.g. of millimeter paper) to reach the required distance d between the CeraPlas® F tip and the substrate surface (see figure 11). The piezobrush® PZ3 is used in countdown mode with treatment time of 10 s.

The test inks gauging the surface energies from 0 to 58 mN/m are typically mixtures of

formamide and ethylene glycol monoethyl ether [24]. Since the ethylene glycol monoethyl ether is much more volatile than the formamide, the proportion of these liquids and consequently the calibration of test ink can change in time. To avoid this parasitic effect, for activation spot visualization, the 58 mN/m test ink consisting of pure formamide is selected. The additional advantage of the value 58 mN/m is, that it assures high dynamic range of the evaluation method, because it is in the middle between the surface energy value of non-treated HDPE (36 mN/m) and the value for the plasma treated surface, which can be up to 72 mN/m.

To assure the accuracy and reproducibility of the activation area determination, the pictures of the ink spot are taken by use of a digital camera with resolution 808 × 576 pixels (approximately 36 pixel/mm^2). The contour of the ink spot is automatically recognized and the ink spot area is calculated from the pixel count by use of a specialized software. The pictures are taken always 10 s after the ink application to avoid the errors due to the temporal variations of the ink spot.

The temperature and humidity have a significant influence on the surface tension of liquids [42]. Therefore, the relative air humidity and the air temperature are measured in the distance of 10 cm from the ink spot and recorded together with the ink area data.

7.2 Influence of the substrate distance

Of high practical importance is the information, in which distance from the treated surface the piezobrush® PZ3 should be held, to achieve the optimum treatment result. To answer this question, the dependence of the activation area on the distance is investigated. The activation area decreases with distance increasing over 3.5 mm (see figure 12). This drop can be explained by three mechanisms: (i) increasing dilution of the chemically active species with increasing distance from the nozzle opening blowing the plasma gases, (ii) the decrease of the reactivity of the short-living chemically active species with flow time,

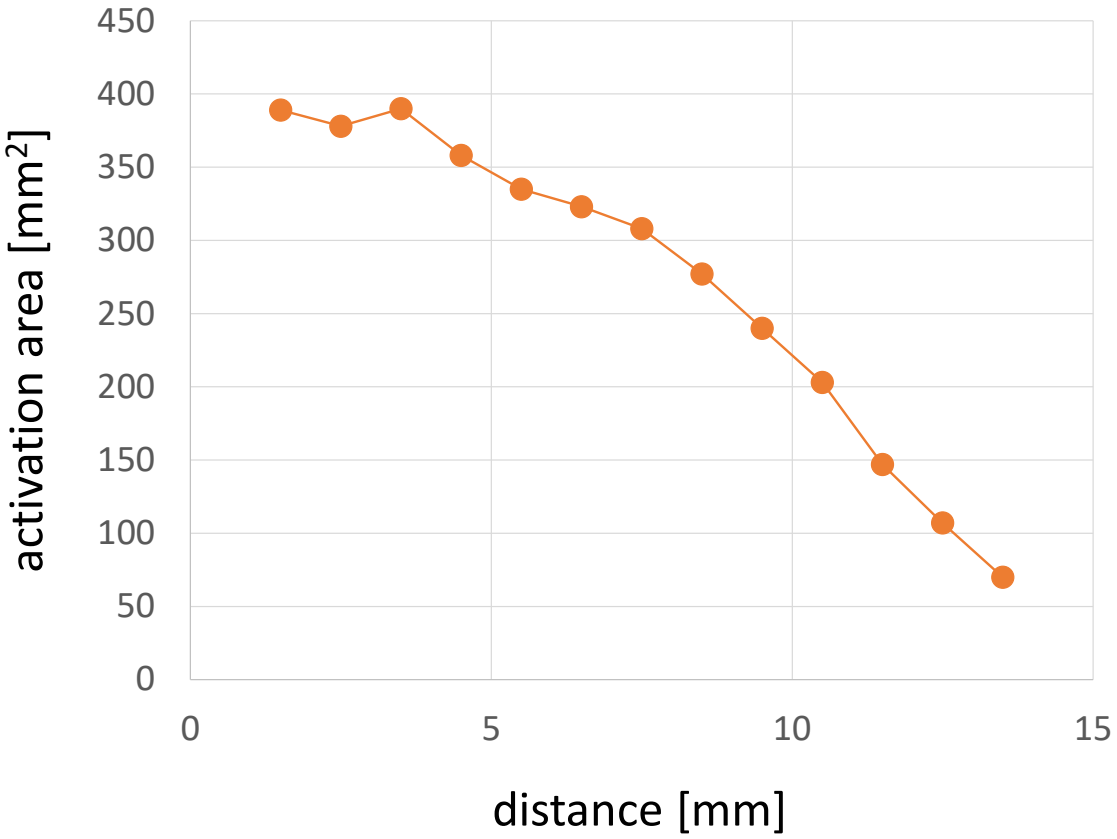

Figure 12: Dependence of the activation area on the distance between the substrate and the tip of the CeraPlas® F.[1] Power level: 100%, treatment time: 10 s.

and (iii) the decrease of the CeraPlas® F electric field with distance from its tip. The maximum of the activation area is reached quite close to the nozzle, 1.5 to 3.5 mm from the CeraPlas® F tip. For distance larger than 13 mm, the activation spot is splitting in two small sub-spots, which can be a criterion for insufficient activation.

7.3 Dependence on the treatment time

A further parameter, which can be set by user, is the treatment time. Intuitively, we expect that the longer the treatment time, the larger the activated area. This expectation is confirmed by a monotonous increase of the activation area with treatment time displayed in figure 13. However, a clear saturation of the area values for longer times is observed. As shown in previous section, the activation area drops strongly with in-

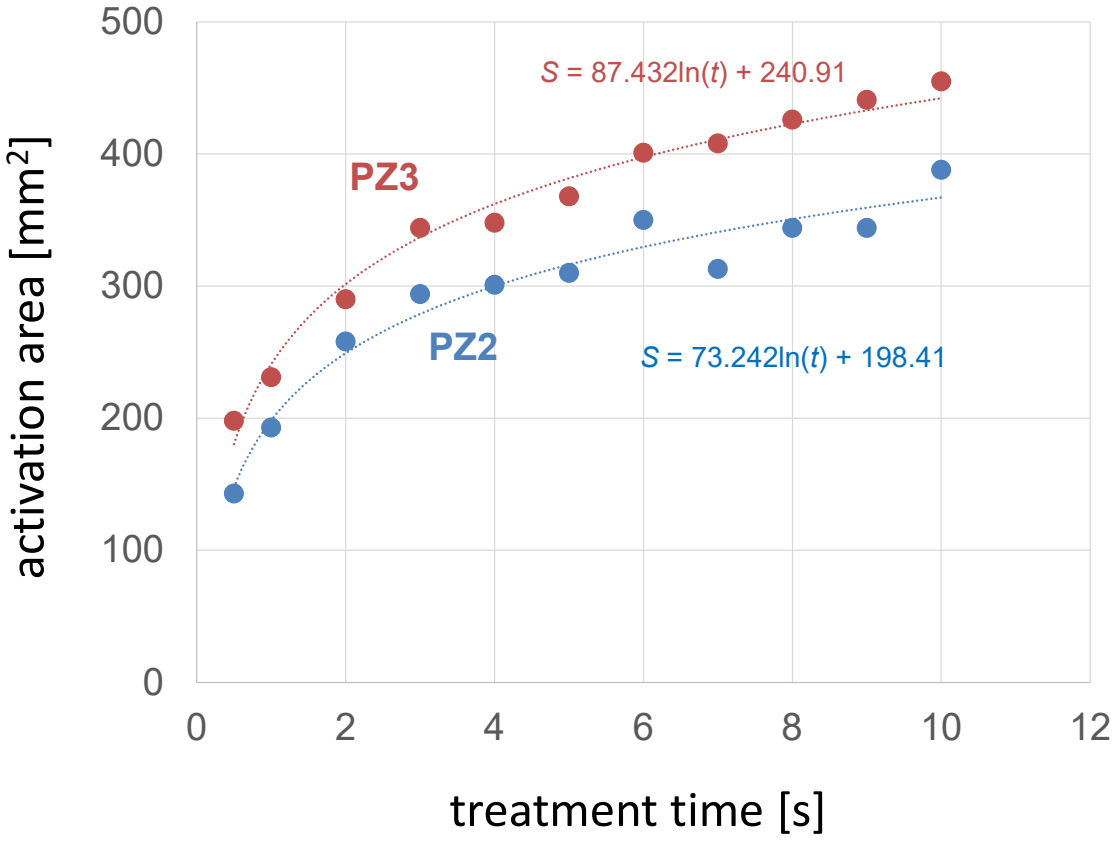

Figure 13: Dependence of activation area on the treatment time for piezobrush® PZ2 and piezobrush® PZ3. The piezobrush® PZ3 power level is 100% (8.0 W). The distance between the tip of CeraPlas® F and the treated surface is 4.5 mm.[1] The activated zone is visualized by 58 mN/m test ink.

creasing axial distance between the tip of the CeraPlas® F and the substrate. All three mechanisms mentioned in section 7.2 are also valid for increase of the radial distance from the CeraPlas® F axis, parallel to the substrate, resulting in limitation of the activated zone size. The maximum size of the activation area typically doesn't exceed 26 mm.

In figure 13, the time dependent activation results of the piezobrush® PZ2 are shown as a blue plot for comparison. The general shape of both plots is very similar, but the activation area for the piezobrush® PZ3 is typically 20-25% larger, than for the piezobrush® PZ2.

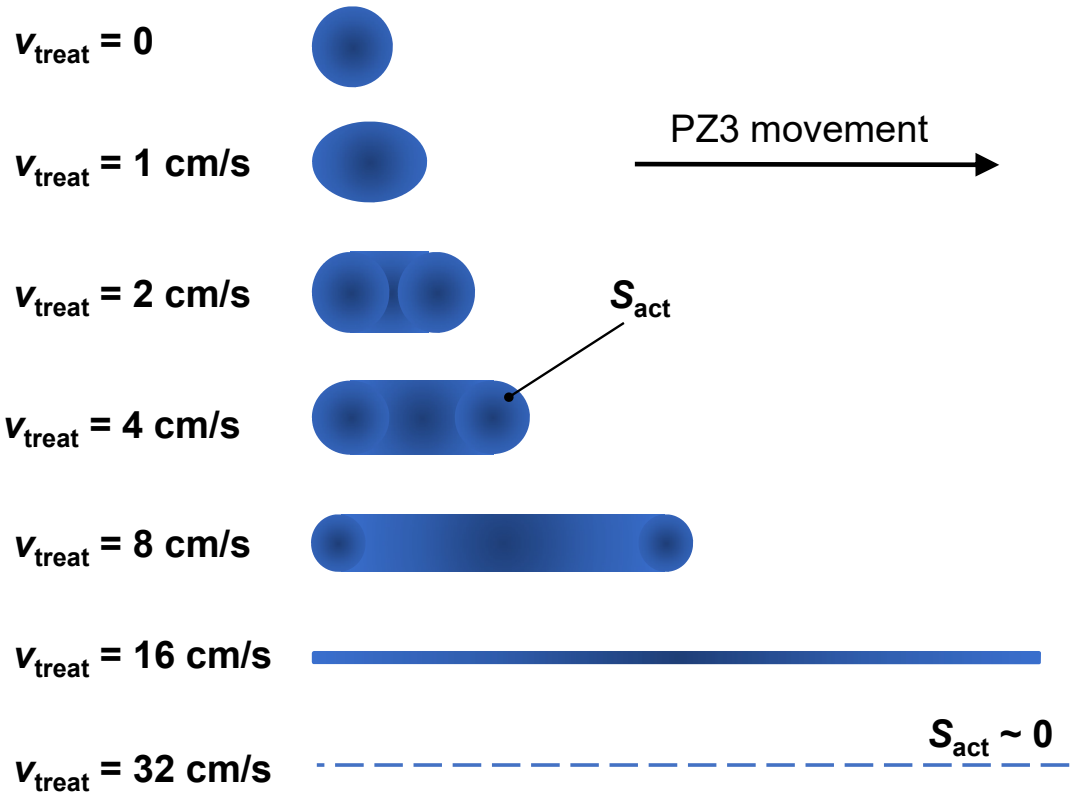

Figure 14: Schematically shown shapes of the activation area after 1 s treatment for different linear speeds v_{treat} of the piezobrush® PZ3.

7.4 Activation rate

Any substrate can be plasma-treated statically or dynamically. The static treatment means, that the relative position of the piezobrush® PZ3 and the substrate is not changing during the plasma-ON time. The dynamic treatment means, that the piezobrush® PZ3 moves with linear speed v_{treat} relative to the substrate during plasma-ON period. The dynamic treatment can be realized either by fixing the piezobrush® PZ3 and moving the substrate e.g. by use of a belt conveyer, or by fixing the substrate and moving the piezobrush® PZ3, e.g. by hand or by xyz-robot. The combination of both kinds of movement can be also applied. For both: static and dynamic plasma treatment, the activation rate η_{act} can be defined as the ratio of the activated area S_{act} to the activation time t_{treat}:

$$\eta_{\mathrm{act}} = \frac{S_{\mathrm{act}}}{t_{\mathrm{treat}}} \tag{4}$$

In figure 14 schematically the shapes of the activation areas for different linear movement speeds of the piezobrush® PZ3 after the same treatment time are shown. The case with $v_{\mathrm{treat}} = 0$ represents the static treatment. For low speeds, the activation area S_{act} and consequently, the activation rate η_{act} increases with increasing speed. Continuing the speed increase, the "plasma trace" gets narrower (e.g. for $v_{\mathrm{treat}} = 8$). For speeds higher than some optimum, the time of interaction between the plasma and the substrate is too short to reach a sufficient activation and the activation area decreases. In the example in figure 14 it occurs for $v_{\mathrm{treat}} = 16$ cm/s. For too high speed, $v_{\mathrm{treat}} = 32$ cm/s in the example, activation vanishes ($S_{\mathrm{act}} \approx 0$). The presented example is strongly simplified. During a real dynamic treatment, the movement speed is not constant, and the shape of activated area is more complex, reflecting the acceleration and deceleration periods.

As demonstrated in the figure 13, the statically produced activation area increases slower than linear with treatment time. Consequently, it can be expected, that the activation rate η_{act} will be higher for shorter treatment times. This expectation is confirmed by the plot in figure 15. The activation rate is about 0.5 cm^2/s for 10 s treatment and increases to 4 cm^2/s for 0.5 s treatment. For some treatment time $0 < t_0 < 0.5$ s, the activation vanishes and the activation rate reaches zero. After time t_{max} fulfilling the condition $t_0 < t_{\mathrm{max}} < 0.5$ s the maximum activation rate η_{max} is reached.

The movement speed of the dynamic treatment can be estimated as:

$$v_{\mathrm{max}} = \frac{L_{\mathrm{act}}}{t_{\mathrm{max}}} \tag{5}$$

where L_{act} is the size of the statical activation patch in the movement direction. For activation patch in shape of a circle, L_{act} is equal its diameter. As shown in figure 10 the

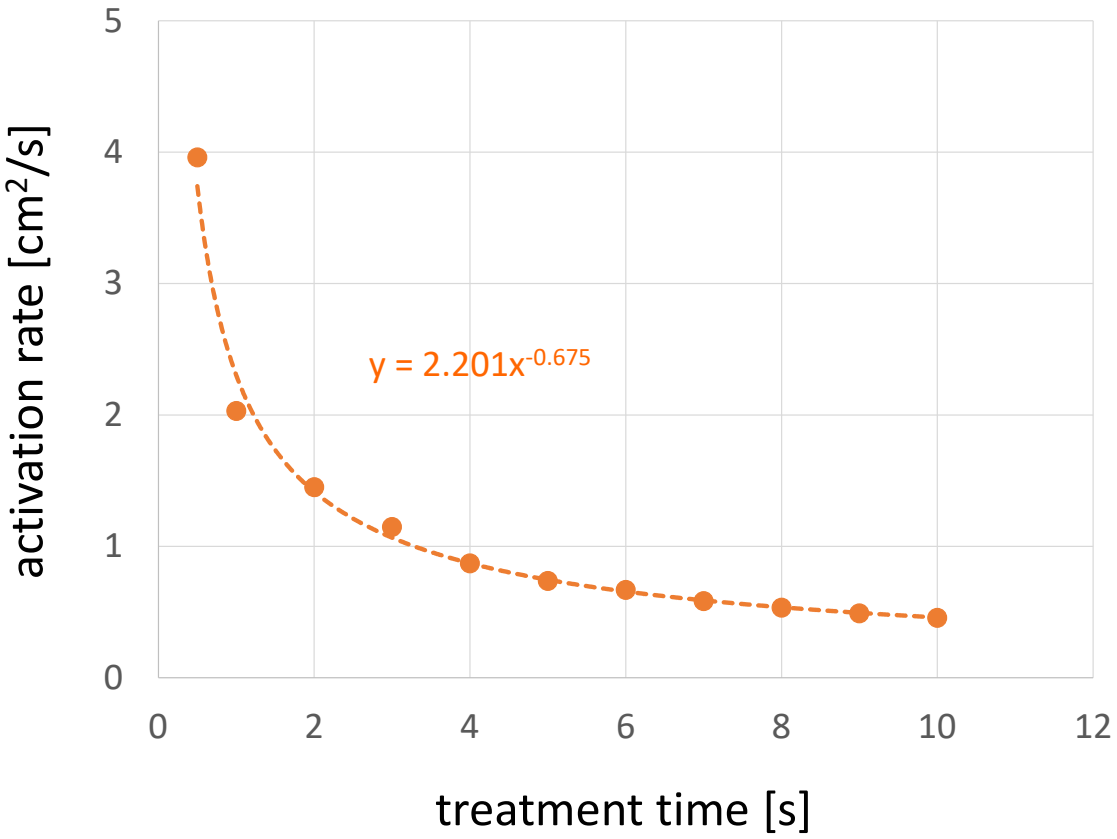

Figure 15: Dependence of the activation rate on the treatment time. The distance between the tip of CeraPlas® F and the treated surface is 4.5 mm.[1] The activated zone is visualized by 58 mN/m test ink.

static activation patch is not rotationally symmetric and L_{act} depends on the azimuthal orientation of the piezobrush® PZ3 during motion. Assuming $L_{\text{act}} = 2$ cm, to reach the maximum activation rate, the piezobrush® PZ2 should be moved with a speed of more than 4 cm/s.

7.5 Influence of the CeraPlas® F input power

In figure 16 dependence of the activation area on the CeraPlas® F power level for open nozzle module is plot in the range from 45 to 100% with 5% steps. The 100% power level corresponds to the CeraPlas® F input power of 8 W. For other nozzle modules, different maximum power value will be valid. The activation area increases almost linearly with power, which correlates with increase of the Ozone concentration, as shown in figure 9.

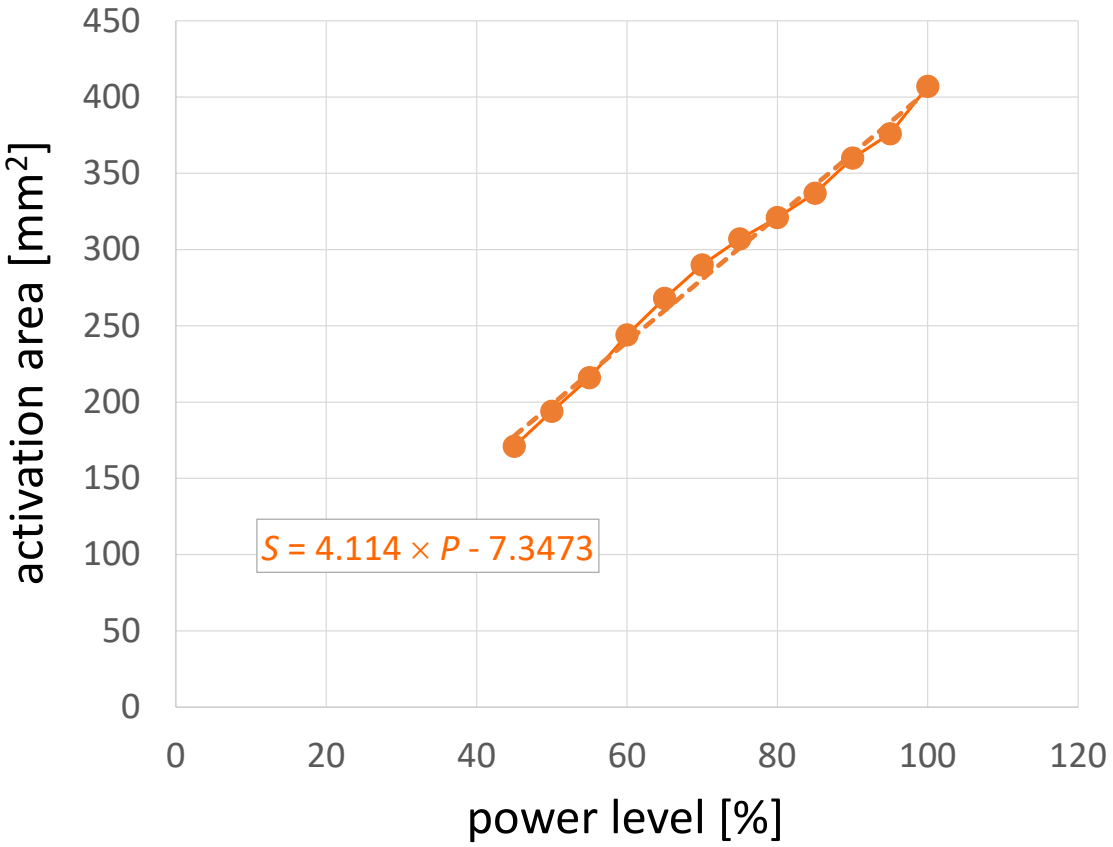

Figure 16: The activation area as a function of the CeraPlas® F input power. The distance between the CeraPlas® F tip and the substrate surface is 4.5 mm.[1] The substrates were treated 10 s.

The growth of the visualized activated area is about 41 mm^2 per 1 W increase of power.

7.6 Influence of the air flow

The air flow in the piezobrush® PZ3 device is increasing with the fan voltage. The activation area as a function of the fan voltage is displayed in fig 17. The red dashed line depicts the fan voltage applied during plasma operation and assuring the sufficient cooling of the CeraPlas® F. A clear tendency can be seen, that the activation area decreases with increasing fan voltage. This can be explained by dilution of the constantly produced amount of the chemically active species in an increasing amount of air, and consequently in less chemistry on the surface, since the transfer processes between the gas flow and the surface depend strongly on the concentration of the chemical species in the gas phase.

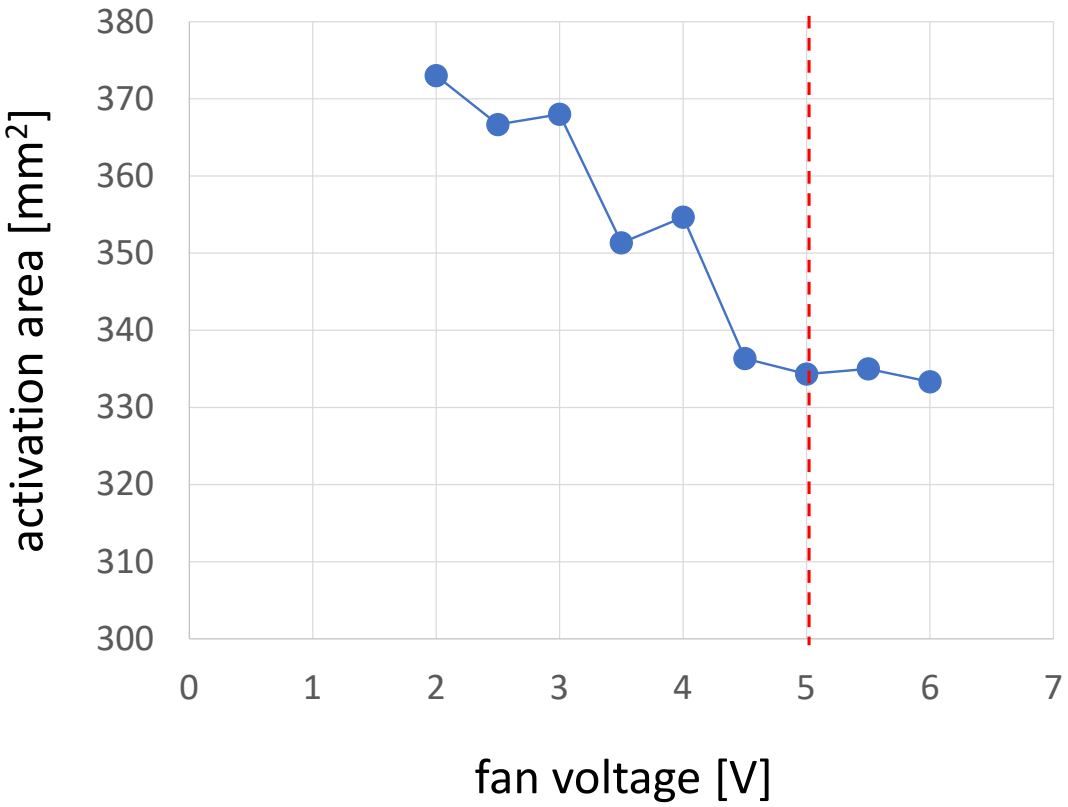

Figure 17: The activation area as a function of the fan voltage. The input power is 8 W. The distance between CeraPlas® F tip and the substrate is 6 mm.[1]

There are numerous factors influencing the air flow and consequently, the working point on the characteristics shown in figure 17. Example can be an obstructing the air flow on the air intake side of the piezobrush® PZ3, or on the plasma side by the construction of the nozzle.

8 Conclusion

The piezobrush® PZ3 is an efficient plasma generator and a very comfortable plasma tool. In comparison with its predecessor piezobrush® PZ2, it reaches 20 - 25% larger activation areas by operation with open nozzle module.

The surface activation is possible in a distance up to 13 mm from the CeraPlas® F tip[1]. But the largest activation area, five times larger than for 13 mm, is reached at the distance of 3.5 mm.

The activation area is linearly increasing with input power of the CeraPlas® F. This increase correlates with the increase of the Ozone production rate and electric field strength.

The piezobrush® PZ3 working with the open nozzle module allows for very reproduceable activation results that are proved to be suitable as a reference for activation area determination.

References

[1] Batakliev, T., Georgiev, V., Anachkov, M., Rakovsky, S., and Zaikov, G. Ozone decomposition. *Interdiscip Toxicol. 7*, 2 (2014), 47 – 59.

[2] Benenson, W., Harris, J. W., Stocker, H., and Lutz, H. *Handbook of physics*. Springer-Verlag New York, Inc., New York, USA, 2002, ch. 8.2, pp. 268 – 278. ISBN 0-387-95269-1.

[3] Benson, S. W., and Axworthy, A. E. Mechanism of the gas phase, thermal decomposition of ozone. *The Journal of Chemical Physics 26*, 6 (1957), 1718 – 1726.

[4] Benwell, A., Kovaleski, S., and Kemp, M. A resonantly driven piezoelectric transformer for high voltage generation. In *2008 IEEE International Power Modulators and High-Voltage Conference* (Las Vegas, NV, USA, May 2008), Institute of Electrical and Electronics Engineers, pp. 113 – 116.

[5] Berg, J., Ed. *Wettability*. Marcel Dekker, Inc., New York, 1993, ch. 1, p. 26.

[6] Borcia, G., Chiper, A., and Rusu, I. Using a He + N_2 dielectric barrier discharge for the modification of polymer surface properties. *Plasma Sources Science and Technology 15* (2006), 849 – 857.

[7] Bronstein, S. *Piezoelectric Transformers in Power Electronics*. PhD thesis, Ben-Gurion University of the Negev, Department of Electrical and Computer Engineering, Beer-Sheva, Israel, 2005.

[8] Büttler, J. R., and Pham, T. Characterization of polyamide 6 - polypropylene laminates. In *AIP Conf. Proc. 2055, Proceedings of the Europe/Africa Conference Dresden 2017 – Polymer Processing Society PPS* (2017), pp. 050008–1–5.

[9] Carazo, A. V. Piezoelectric transformers: An historical review. *Actuators 5* (2016), 1 – 22.

[10] Daumont, D., Brion, J., Charbonnier, J., and Malicet, J. Ozone UV spectroscopy I: Absorption cross-section at room temperautre. *Journal of Atmospheric Chemistry 15* (1992), 145 – 155.

[11] Day, M., and Lee, B. S. Understanding piezoelectric transformers in CCFL backlight applications. *Analog Applications Journal 4Q* (2002), 12 – 8.

[12] Dhandapani, B., and Oyama, S. Gas phase ozone decomposition catalysts. *Applied Catalysis B: Environmental 11* (1997), 129 – 166.

[13] Dorai, R., and Kushner, M. J. A model for plasma modification of polypropylene using atmospheric pressure discharges. *J. Phys. D: Appl. Phys. 36* (2003), 666 – 685.

[14] Eliasson, B., Hirth, M., and Kogelschatz, U. Ozone synthesis from oxygen in dielectric barrier discharges. *J. Phys. D: Appl. Phys. 20* (1987), 1421 – 37.

[15] Engemann, J., and Teschke, M. Device for producing an atmospheric pressure plasma, May 14 2009. US Patent Application US 2009/0122941 A1.

[16] EPCOS AG. Evaluation kit CeraPlas® HF Driver for CeraPlas® series. `https://www.mouser.de/datasheet/2/400/ceraplas-driving-circuit-user-guide-1487527.pdf`, 4 2018. Data sheet.

[17] Fridman, A. *Plasma Chemistry.* Cambridge University Press, New York, 2008, pp. 387 – 388.

[18] Fridman, A. *Plasma Chemistry.* Cambridge University Press, New York, 2008, pp. 389 – 390.

[19] Fukunaga, H., Kakehashi, H., Ogasawara, H., and Ohta, Y. Effect of dimension on characteristics of Rosen-type piezoelectric transformer. In *Power Electronics Specialists Conference, 1998. PESC 98 Record. 29th Annual IEEE Volume: 2* (1998), Institute of Electrical and Electronics Engineers, pp. 1504 – 1510.

[20] Gardoni, D., Vailati, A., and Canziani, R. Decay of ozone in water: A review. *Ozone: Science & Engineering 34* (2012), 233 – 242.

[21] Hooker, M. W. Properties of PZT-based piezoelectric ceramics between -150 and 250°C. Tech. Rep. NASA/CR-1998-208708, National Aeronautics and Space Administration - NASA, USA, 1998.

[22] Hsu, Y.-H., Lee, C.-K., and Hsiao, W.-H. Optimizing piezoelectric transformer for maximum power transfer. *Smart Materials and Structures 12*, 3 (2003), 373.

[23] Hutsel, B. T. *Characterization of a piezoelectric transformer plasma source*. PhD thesis, University of Missouri, Faculty of the Graduate School, Jesse Hall, 801 Conley Ave, Columbia, MO 65211, USA, 2012.

[24] International, A. Standard test method for wetting tension of polyethylene and polypropylene films. `http://www.astm.org`, 3 2004. Designation: D 2578 – 04.

[25] Ito, Y., Okawa, T., Fujii, T., and Tanaka, M. Influence of plasma treatment on surface properties of zirconia. *J. Osaka Dent. Univ. 50*, 2 (2016), 79 – 84.

[26] Ito, Y., Okawa, T., Fukumoto, T., Tsurumi, A., Tatsuta, M., Fujii, T., Tanaka, J., and Tanaka, M. Influence of atmospheric pressure low-temperature plasma treatment on the shear bond strength between zirconia and resin cement. *Journal of Prosthodontic Research 60*, 4 (2016), 289 – 293.

[27] Itoh, H., Teranishi, K., and Suzuki, S. Discharge plasmas generated by piezoelectric transformers and their applications. *Plasma Sources Sci. Technol. 15*, 2 (2006), S51.

[28] Kemmerling, S., Ziegler, J., Schweighauser, G., Arnold, S. A., Giss, D., Müller, S. A., Ringler, P., Goldie, K. N., Goedecke, N., Hierlemann, A., Stahlberg, H., Engel, A., and Braun, T. Connecting μ-fluidics to electron microscopy. *Journal of Structural Biology 177*, 1 (2012), 128 – 134.

[29] Kim, H., Brockhaus, A., and Engemann, J. Atmospheric pressure argon plasma jet using a cylindrical piezoelectric transformer. *Applied Physics Letters 95*, 21 (2009), 211501.

[30] Küchler, A. *High Voltage Engineering: Fundamentals - Technology - Applications*. Springer Vieweg, Berlin – Heidelberg, 2017, ch. 3.2, p. 187.

[31] Lin, C.-Y. *Design and Analysis of Piezoelectric Transformer Converters*. PhD thesis, Virginia Polytechnic Institute and State University, Blacksburg, Virginia, 1997.

[32] Lin, R.-L. *Piezoelectric Transformer Characterization and Application of Electronic Ballast*. PhD thesis, Virginia Polytechnic Institute and State University, Blacksburg, Virginia, USA, 2001.

[33] Lo, Y.-K., Lin, C.-H., and Pai, K.-J. Design and analysis of a piezoelectric transformer-based half-bridge resonant inverter for CCFL backlight modules. In *IEEE International Symposium on Industrial Electronics, ISIE 2006, Montréal, Québec, Canada* (July 9-12, 2006), Institute of Electrical and Electronics Engineers, pp. 892 – 896.

[34] Martin, T., Pigache, F., Nadal, C., and Callegari, T. Experimental analysis of piezoelectric plasma discharge generator. In *2012 IEEE International Ultrasonics Symposium* (Oct 2012), Institute of Electrical and Electronics Engineers, pp. 1 – 5.

[35] Matsumi, Y., and Kawasaki, M. Photolysis of atmospheric ozone in the ultraviolet region. *Chemical Reviews 103*, 12 (2003), 4767 – 4782. PMID: 14664632.

[36] McClurkin, J., and Maier, D. Half-life time of ozone as a function of air conditions and movement. In *10th International Working Conference on Stored Product Protection*. Julius-Kühn-Archiv, Estoril, Portugal, 27 June–2 July, 2010, pp. 381 – 385.

[37] Molina, L. T., and Molina, M. J. Absolute absorption cross sections of ozone in the 185- to 350-nm wavelength range. *J. Geophys. Research 91*, D13 (1986), 14,501 – 14,508.

[38] Moulson, A., and Herbert, J. *Electroceramics, 2nd ed.* John Wiley & Sons Ltd,, The Atrium, Southern Gate, Chichester, West Sussex PO19 8SQ, England, 2003.

[39] Nettesheim, S., Korzec, D., Burger, D., Kuegerl, G., Puff, M., and Hoppenthaler, F. Apparatus for producing a plasma and hand-held device having the apparatus, 10 2017. US Patent 9,788,404 B2.

[40] Neuhaus, S. *Functionalization of Polymer Surfaces with Polyelectrolyte Brushes.* PhD thesis, ETH Zürich, Zürich, Switzerland, 2011.

[41] Neuhaus, S., Padeste, C., and Spencer, N. D. Functionalization of fluropolymers and polyolefins via grafting of polyelectrolyte brushes from atmospheric-pressure plasma activated surfaces. *Plasma Processes and Polymers 8*, 6 (2011), 512 – 522.

[42] Pérez-Díaz, J. L., Álvarez-Valenzuela, M. A., Valiente-Blanco, I., Jimenez-Lopez, S., Palacios-Cuesta, M., Garcia, O., Diez-Jimenez, E., Sanchez-Garcia-Casarrubios, J., and Cristache, C. On the influence of relative humidity on the contact angle of a water droplet on a silicon wafer. In *Proceedings of ASME, Paper number IMECE2013-63781* (November 15-21, San Diego, California, USA, 2013).

[43] Razumovsky, S., Gorshenev, V., Kovarskii, A., and Shchegolikhin, A. Dynamics and mechanism of the interaction of graphite powders with ozone. *Russian Chemical Bulletin, International Edition 57*, 9 (2008), 1806 – 1810.

[44] Relyon Plasma GmbH. Operating instructions for piezobrush® PZ3 hand-held device and piezobrush® PZ3 professional set, BA-PZ3_ML / F0354400 EN.

https://www.relyon-plasma.com/wp-content/uploads/2020/04/F0354400_BA_piezobrush_PZ3_Handger%C3%A4t_EN.pdf, 2020. [Online; accessed 12-Oct-2020].

[45] Rosen, C. A., Fish, K. A., and Rothenberg, H. C. Electromechanical transducer, 8 1958. US Patent 2,830,274.

[46] Smidt, P. J. M., and Duarte, J. L. Powering neon lamps through piezoelectric transformers. In *Proc. of 27th Annual IEEE Power Electronics Specialists Conference - PESC'96* (1996), Institute of Electrical and Electronics Engineers, pp. 310 – 315.

[47] Sotelo, J., Bltrán, F., Benítez, F., and Bltrán-Heredia, J. Ozone decomposition in water: Kinetic study. *Ind. Eng. Chem. Rev. 26*, 26 (1987), 39 – 43.

[48] Stawarczyk, B., Thrun, H., Eichberger, M., Roos, M., Edelhoff, D., Schweiger, J., and Schmidlin, P. R. Effect of different surface pretreatments and adhesives on the load-bearing capacity of veneered 3-unit PEEK FDPs. *Zurich Open Repository and Archive*, JPD-14-751 (2015), 1 – 25.

[49] Su, Y.-H. *Power Enhancement of Piezoelectric Technology based Power Devices by Using Heat Transfer Technology*. PhD thesis, L'Ecole Normale Superieure de Cachan, 94235 Cachan Cedex, France, 2014.

[50] TDK Electronics. Cold plasma from a single component. https://www.tdk-electronics.tdk.com/en/373562/tech-library/articles/applications---cases/applications---cases/cold-plasma-from-a-single-component/1109546, 31 2014. Applications & Cases.

[51] TDK Electronics AG. CeraPlas^{TM} series. piezoelectric transformer designed for gas ignition & plasma generation. Data sheet, 2019. Type CP7006K20T1000.

[52] Teranishi, K., Shimomura, N., Suzuki, S., and Itoh, H. Development of dielectric barrier discharge-type ozone generator constructed with piezoelectric transformers: effect of dielectric electrode materials on ozone generation. *Plasma Sources Sci. Technol. 18*, 4 (2009), 045011.

[53] Teschke, M. Piezoelectric low voltage atmospheric pressure plasma sources. *Contributions to Plasma Physics 49*, 9 (2009), 614 – 623.

[54] Teschke, M. *Piezoelektrisch betriebene Niederspannungs- Atmosphärenduck-Plasmaquellen*. PhD thesis, Bergische Universität Wuppertal, Wuppertal, Germany, 2009.

[55] Teschke, M., and Engemann, J. Low voltage app-generation by piezo ceramics: A new (r)evolutionary enabling technology. In *Proc. 18th Int. Symp. Plasma Chem. (ISPC)* (August 2007), pp. 1 – 4.

[56] Teschke, M., and Engemann, J. Low voltage APP-generation by piezo ceramics: Basic structures, electro-mechanical simulations and poling techniques. In *Proc. 18th Int. Symp. Plasma Chem. (ISPC)* (August 2007), pp. 1 – 4.

[57] Ujino, D., Nishizaki, H., Higuchi, S., Komasa, S., and Okazaki, J. Effect of plasma treatment of titanium surface on biocompatibility. *Appl. Sci. 9, 2257* (2019), 1 – 12.

[58] Wells, E. Comparing magnetic and piezoelectric transformer approaches in CCFL applications. *Analog Applications Journal 1Q* (2002), 12 – 18.

[59] Wikipedia. Piezoelectric direct discharge plasma. `https://en.wikipedia.org/wiki/Piezoelectric_direct_discharge_plasma`, 2016. [Online; accessed 17-Oct-2016].